Virology 433 (2012) 421–430

Contents lists available at SciVerse ScienceDirect

Virology

journal homepage: www.elsevier.com/locate/yviro

Characterization of cellular furin content as a potential factor determining the susceptibility of cultured human and animal cells to coronavirus infectious bronchitis virus infection

Felicia P.L. Tay [1], Mei Huang [1], Li Wang, Yoshiyuki Yamada, Ding Xiang Liu *

School of Biological Sciences, Nanyang Technological University, 60 Nanyang Drive, Singapore 637551, Singapore

ARTICLE INFO

Article history:
Received 29 May 2012
Returned to author for revisions
25 June 2012
Accepted 27 August 2012
Available online 18 September 2012

Keywords:
Coronavirus infectious bronchitis virus
Human and animal cell lines
Susceptibility
Furin
Spike protein

ABSTRACT

In previous studies, the Beaudette strain of coronavirus infectious bronchitis virus (IBV) was adapted from chicken embryo to Vero, a monkey kidney cell line, by serial propagation for 65 passages. To characterize the susceptibility of other human and animal cells to IBV, 15 human and animal cell lines were infected with the Vero-adapted IBV and productive infection was observed in four human cell lines: H1299, HepG2, Hep3B and Huh7. In other cell lines, the virus cannot be propagated beyond passage 5. Interestingly, cellular furin abundance in five human cell lines was shown to be strongly correlated with productive IBV infection. Cleavage of IBV spike protein by furin may contribute to the productive IBV infection in these cells. The findings that IBV could productively infect multiple human and animal cells of diverse tissue and organ origins would provide a useful system for studying the pathogenesis of coronavirus.

Introduction

Entry of viruses into host cells by crossing the plasma membrane is an essential step for successful viral replication. This process is initially mediated by the interaction of a viral protein with its corresponding host cell receptor(s). This interaction is therefore one of the prime determinants for the host cell specificity of a virus. Cellular receptors identified for coronavirus, important pathogens of human and many other animal species, include aminopeptidase N (APN) for alphacoronaviruses transmissible gastroenteritis virus (TGEV), human coronavirus (HCoV) 229E, canine coronavirus (CCoV) and feline infectious peritonitis virus (FIPV) (Delmas et al., 1992; Tresnan et al., 1996; Yeager et al., 1992), the carcinoembryonic antigen–cell adhesion molecular (CEACAM) for mouse hepatitis virus (MHV) (Coutelier et al., 1994; Dveksler et al., 1991; Godfraind et al., 1995; Williams et al., 1991), and angiotensin-converting enzyme 2 (ACE2) and CD209L for severe acute respiratory syndrome coronavirus (SARS-CoV) and HCoV-NL63 (Hofmann et al., 2005; Jeffers et al., 2004; Li et al., 2003). CD209L was initially identified as an attachment factor for human immunodeficiency virus (Curtis et al., 1992; Geijtenbeek et al., 2000), but was subsequently found to be a co-receptor for hepatitis C virus (Pohlmann et al., 2003), cytomegalovirus (Halary et al., 2002), dengue virus (Tassaneetrithep et al., 2003) and SARS-CoV (Jeffers et al., 2004).

Coronavirus infectious bronchitis virus (IBV), a prototype coronavirus, is the etiological agent of infectious bronchitis which impairs the respiratory and urogenital tracts of chicken (Cavanagh, 2007). The receptor(s) for IBV in its native or adapted host cells remains unknown, although IBV might use APN as a receptor in vitro (Miguel et al., 2002). In addition, the widely distributed sialic acid was suggested to be important for the primary attachment of IBV to host cells (Winter et al., 2006). In a more recent paper, DC-SIGN-like lectins, including L-SIGN, were shown to be able to increase susceptibility to infection by IBV in otherwise refractory cells (Zhang et al., 2012).

In a recent study, furin was shown to be responsible for proteolytic activation of S protein at a novel $RRRR_{690}$/S motif in the S2 region (Yamada and Liu, 2009). This cellular proprotein convertase is a calcium-dependent serine protease that circulates between *trans*-Golgi network (TGN), plasma membrane, and early endosome by association with exocytic and endocytic pathways (Bosshart et al., 1994; Molloy et al., 1994). It cleaves a wide variety of protein precursors after the C-terminal arginine (R) residue in the preferred consensus motif (RXR(K)R/R (K, lysine; X, any amino acid). Introduction of mutations into the $RRRR_{690}$/S motif and use of specific furin inhibitors demonstrated that furin may play an important role in furin-dependent entry, cell–cell fusion and infectivity of IBV in cultured cells (Yamada and Liu, 2009). Similar observations were also reported by Belouzard et al. (2009).

* Corresponding author.
E-mail address: dxliu@ntu.edu.sg (D. Xiang Liu).
[1] Equal contributors.

0042-6822/$ - see front matter © 2012 Elsevier Inc. All rights reserved.
http://dx.doi.org/10.1016/j.virol.2012.08.037

Coronaviruses generally have a limited host range. However, recent evidence showed that several coronaviruses could break the host barrier and become zoonotic. For example, the novel SARS-CoV was found to cross host species from animal to human (Guan et al., 2003). HCoV-OC43 could infect cells from a large number of mammalian species, although the virus was propagated exclusively in suckling mouse brains (Butler et al., 2006). To study the mechanisms underlying the host cell specificity and susceptibility to coronavirus and coronavirus–host interactions, the Beaudette strain of IBV was adapted from chicken embryo to a monkey kidney cell line, Vero, by continuous propagation for 65 passages (Shen et al., 2003, 2004). This adaptation was accompanied by mutations in the spike (S) protein (Fang et al., 2005, 2007). In this study, infection of 15 cell lines of different species and tissue origins with the Vero cell-adapted IBV shows that four out of the 15 cell lines were able to support continuous and productive IBV infection with high efficiency. Meanwhile, strong correction between cellular furin abundance and productive IBV infection was found in five human cell lines infected with IBV.

Results

Susceptibility of different human and animal cell lines to Vero-adapted IBV

The susceptibility of 15 human and animal cell lines to IBV infection was tested by infecting cells with the 65th passage (p65) of Vero-adapted IBV. The tissue and species origins of these cell lines are listed in Table 1. Based on the preliminary observations from pilot tests, the susceptibility of these cells to IBV could be divided into two groups, the more susceptible and the more resistant groups. The more susceptible cell lines, including H1299, Huh7, HepG2, Hep3B and HCT116, were infected with IBV at a multiplicity of infection of approximately 0.1 and harvested at 0, 12, 16, 24, 36 and 48 h post-infection, respectively. The more resistant cells, including A549, MRC-5, DLD-1, DLD-1Amix, CHO, U937, HeLa, BHK-21, 293T, and Cos-7, were infected with IBV at a multiplicity of infection of approximately 0.3, a higher MOI to ensure successful infection of these cells, and harvested at the same time points as the former group.

The results showed that almost all cell lines tested could be infected by virus stocks prepared from IBV-infected Vero cells in passage 1. These cells were then continuously infected with the freezing/thawing preparations of IBV from the same cell lines infected with IBV. IBV was found to be able to propagate efficiently to at least passage 20 (p20) only in four lines derived from human cancer cells, i.e., H1299, Huh7, Hep3B and HepG2 (Table 1). In other cell lines, viral infectivity was found to be lost in passages 2–5 (Table 1). Fig. 1a–c shows the expression of IBV nucloecapsid (N) protein in the 15 cell lines infected by passages 1–3 of IBV, which were harvested at 24 h post-infection. One exception is HCT116 cell line, in which productive infection with low efficiency was observed after 20 passages (Table 1).

Table 1
Continuous propagation of IBV in 16 susceptible cell lines.

Cell line	Tissue	Organism	Productive infection[a]
H1299	Lung	Human	Yes
A549	Lung	Human	No
MRC-5	Lung	Human	No
Huh7	Liver	Human	Yes
HepG2	Liver	Human	Yes
Hep3B	Liver	Human	Yes
HCT116	Colorectal	Human	Yes/no
DLD-1	Colorectal	Human	No
DLD-1A	Colorectal	Human	No
Vero	Kidney	Monkey	Yes
BHK	Kidney	Hamster	No
293T	Kidney	Human	No
Cos-7	Kidney	Monkey	No
CHO	Ovarian	Hamster	No
HeLa	Cervical	Human	No
U937	Blood	Human	No

[a] Continuous propagation of IBV up to at least 20 passages.

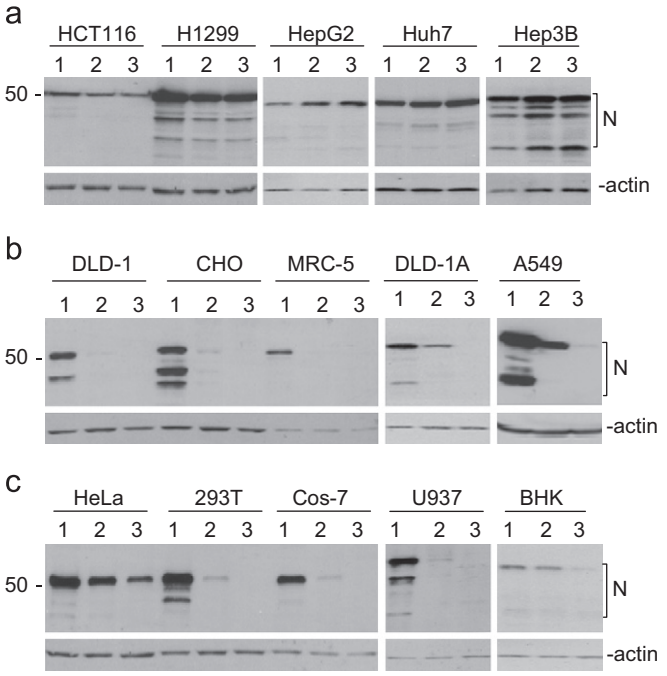

Fig. 1. Infection of 15 human and animal cell lines with IBV. (a) Western blot analysis of the expression of IBV N protein in IBV-infected HCT116, H1299, HepG2, Huh7 and Hep3B cells. Cells were infected with passages 1–3 of IBV and harvested at 24 h post-infection. Cell lysates were prepared and separated on SDS-10% polyacrylamide gels. The expression of IBV N protein was analyzed by Western blot with anti-N antibodies, after the proteins were separated by SDS-PAGE. The membrane was also probed with anti-actin monoclonal antibody as a loading control. (b) Western blot analysis of the expression of IBV N protein in IBV-infected DLD-1, CHO, MRC-5, DLD-1A and A549 cells. Cells were infected with passages 1–3 of IBV and harvested at 24 h post-infection. Cell lysates were prepared and separated on SDS-10% polyacrylamide gels. The expression of IBV N protein was analyzed by Western blot with anti-N antibodies, after the proteins were separated by SDS-PAGE. The membrane was also probed with anti-actin monoclonal antibody as a loading control. (c) Western blot analysis of the expression of IBV N protein in IBV-infected HeLa, 293T, Cos-7, U937 and BHK cells. Cells were infected with passages 1–3 of IBV and harvested at 24 h post-infection. Cell lysates were prepared and separated on SDS-10% polyacrylamide gels. The expression of IBV N protein was analyzed by Western blot with anti-N antibodies, after the proteins were separated by SDS-PAGE. The membrane was also probed with anti-actin monoclonal antibody as a loading control.

Characterization of viral structural protein expression and syncytium formation in productive IBV infection of six human and animal cell lines

The expression kinetics of IBV structural proteins, S, membrane (M) and N, in H1299, Huh7, Hep3B, HepG2 and HCT116 cells were analyzed by Western blot with polyclonal antibodies. As a positive control, Vero cells were first infected with IBV at a multiplicity of infection of approximately 1 and analyzed. As shown in Fig. 2a, analysis of IBV-infected Vero cells with anti-S antibodies detected the full-length glycosylated (S*), the full-length unglycosylated (S) and the S1/S2 cleavage forms of the protein from 12 h post-infection. Analysis of the same cell lysates with anti-N antibodies detected the full-length N protein (N) from

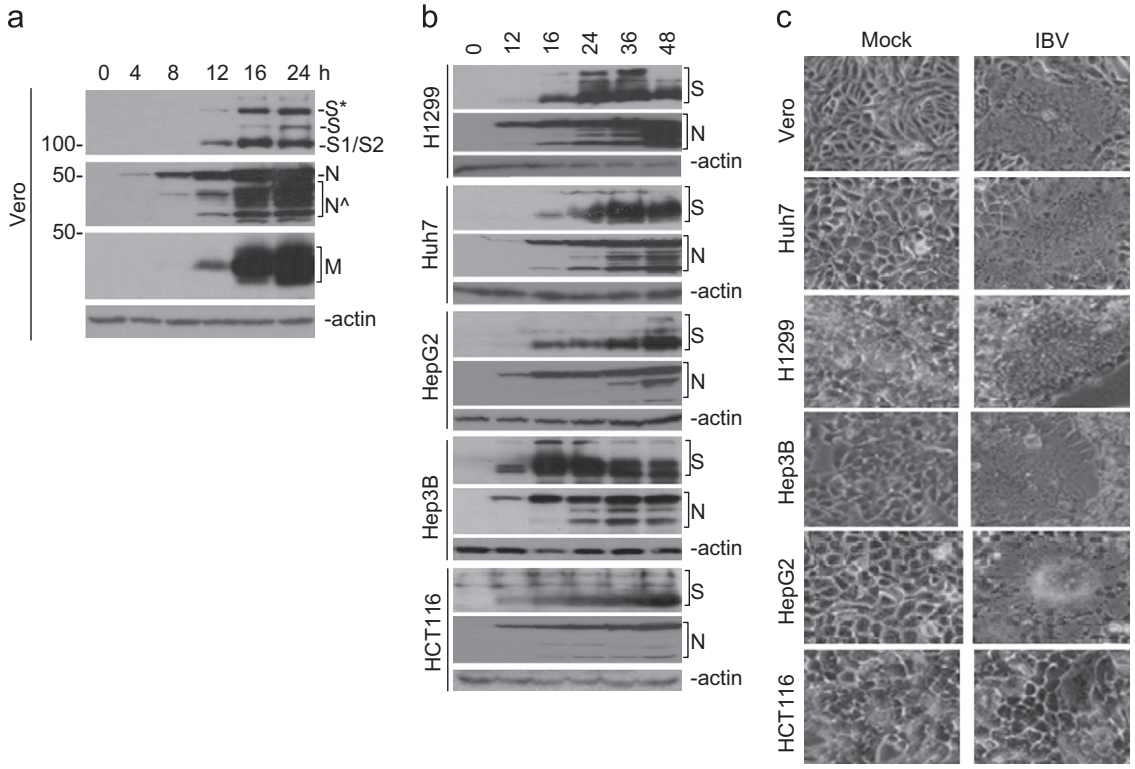

Fig. 2. Viral structural protein expression and syncytium formation in productive IBV infection of five human and animal cell lines. (a) Western blot analysis of the expression of IBV S, M and N proteins in IBV-infected Vero cells. Vero cells were infected with IBV at a multiplicity of infection of approximately 1 and harvested at 0, 4, 8, 12 and 24 hours post-infection, respectively. Cell lysates were prepared and separated on SDS-10% polyacrylamide gels. The expression of IBV S, N and M proteins was analyzed by Western blot with anti-S, -N and -M antibodies, respectively, after the proteins were separated by SDS-PAGE. The full-length glycosylated (S*), the full-length unglycosylated (S) and the S1/S2 cleavage forms of the S protein are labeled. Also indicated are the full-length N protein (N) and several more-rapidly-migrating bands (N^). Both glycosylated and unglycosylated M protein were labeled as M. The membrane was also probed with anti-actin monoclonal antibody as a loading control. (b) Analysis of IBV infection in H1299, Huh7, HepG2, Hep3B and HCT116. Cells were infected with IBV and harvested at 0, 12, 16, 24, 36, and 48 h post-transfection. Cell lysates were prepared and separated on SDS-10% polyacrylamide gels. The expression of IBV S and N proteins was analyzed by Western blot with anti-S and -N antibodies, respectively, after proteins were separated by SDS-PAGE. The membranes were also probed with anti-actin monoclonal antibody as loading controls. (c) Cytopathic effect of Vero, Huh7, H1299, Hep3B, HepG2 and HCT116 cells infected with the Vero-adapted IBV. Cells were infected with IBV at a multiplicity of infection of approximately 0.1 and observed with phase-contrast microscopy at 12–24 h post-infection.

8 h post-infection, in addition to several more-rapidly-migrating bands (N^) (Fig. 2a) representing either cleavage or premature termination products of N protein (Li et al., 2005). The same lysates were also probed with anti-M antibodies, showing the expression of M protein from 12 h post-infection (Fig. 2a). As both M and S showed similar expression kinetics, analysis of only S and N proteins was conducted in other IBV-infected cells in the subsequent studies.

Efficient IBV infection, as observed by Western blot analysis with anti-S and anti-N antibodies, was detected in four human cell lines, H1299, Huh7, HepG2 and Hep3B infected with the Vero-adapted IBV (Fig. 2b). Consistent with the weak productive infection observed during continuous passages of IBV in HCT116 cells, the accumulation of S and N proteins was much slower in this cell line over the time-course, compared to that in the other cell lines (Fig. 2b). It was also noted that the patterns of S protein cleavage and processing were slightly different from cell line to cell line (Fig. 2b). As these patterns were not consistently observed in a given cell line in repeated experiments (data not shown), it is unlikely that they may reflect differences in post-translational modification and processing of the protein in a given cell line.

The cytopathic effect (CPE) caused by IBV infection in these cells was also visually examined by microscopy at 12–24 h post-infection. Similar to that in Vero cells, infection of H1299, Huh7, HepG2 and Hep3B cells with IBV generated giant syncytia at 12–24 h post-infection, leading to the destruction of the entire monolayers and death of the infected cells afterwards (Fig. 2c). However, syncytium formation was not observed in HCT116 cells (Fig. 2c). Instead, the infected cells were rounded up and lysed eventually (Fig. 2c). As productive infection was consistently observed in these cell lines, we would refer the infection of IBV in these cell lines (as well as in Vero cells) as productive IBV infection subsequently in this study.

Growth properties and stability of IBV in H1299, Huh7 and HCT116 cells

The growth kinetics of p1, p5 and p20 viruses collected from IBV-infected H1299 and Huh7 cells were characterized. As IBV infection of the three cell lines of human hepatoma origin, Huh7, HepG2 and Hep3B cells, showed similar kinetics in terms of growth and protein synthesis, only Huh7 cells were chosen for this study. Analysis of the growth kinetics of p1, p5, and p20 from H1299 and Huh7 showed similar growth kinetics as in Vero cells (Fig. 3a–c). Viruses reached their peak titer at 16–24 h post-infection and declined afterwards (Fig. 3b and c).

These growth curves indicated that the infectivity of Vero-adapted IBV did not change much during propagation in human cells, suggesting that the virus readily infected human cells without requirement for further adaptation. To confirm this possibility, the genetic stability of IBV in H1299 and Huh7 cells was tested by sequencing the S gene from plaque-purified as well as unpurified p1, p5 and p20 passages. Only one silent mutation from ATT (Ilu) to ATC (Ilu) at the nucleotide position 23565 was found in the S2 region of two isolates from Huh7-p5. The occurrence of rare and inconsistent

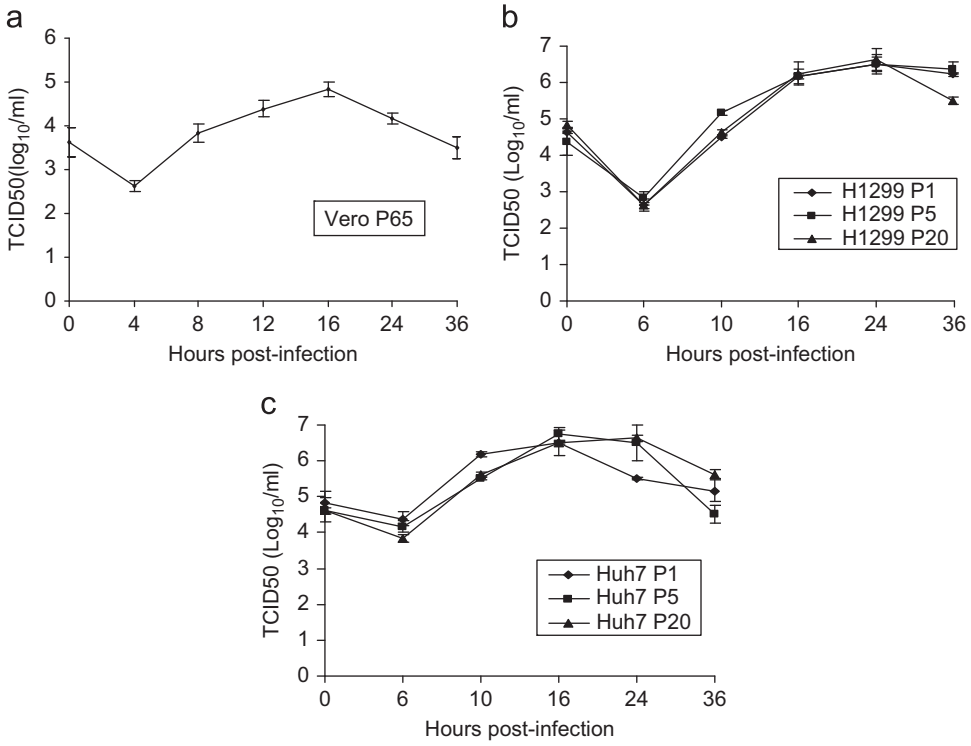

Fig. 3. Growth curves of passages 1, 5 and 20 of IBV in H1299 and Huh7 cells. (a) Vero cells were infected with IBV and harvested at 0, 4, 8, 12, 16, 24 and 36 h post-infection, respectively. Cells were lysed by freezing and thawing three time and viral titers were determined by TCID50 assay on Vero cells. (b) H1299 cells were infected with H1299-p1, H1299-p5 and H1299-p20, respectively, and harvested at 0, 6, 10, 16, 24 and 36 h post-infection, respectively. Cells were lysed by freezing and thawing three times and viral titers were determined by TCID50 assay on Vero cells. (c) Huh7 cells were infected with Huh7-p1, Huh7-p5 and Huh7-p20, respectively, and harvested at 0, 6, 10, 16, 24 and 36 h post-infection. Cells were lysed by freezing and thawing three times and viral titers were determined by TCID50 assay on Vero cells.

mutations in the S gene confirms that the Vero-adapted IBV is genetically stable during passaging in human cell lines.

Correlation between productive IBV infection and cellular furin abundance in Huh7, H1299, HeLa, A549 and 293T cells

The observation that IBV could infect most cell lines tested in passage 1 but lost infectivity in subsequent passages in some cell lines suggests that the cellular restriction point(s) may exist at some late stages of the viral life cycle during primary infection and early stages during secondary infection, probably at the release of progeny viruses and spread of infection to neighboring cells. In a previous study, a novel furin site is identified in the IBV S protein that is essential for furin-dependent entry, syncytium formation and infectivity of IBV in cultured cells (Yamada and Liu, 2009). It prompted us to examine the cellular content of furin in these cells. Western blotting analysis of Huh7, H1299, HeLa, 293T and A549 cells showed differential expression of furin (Fig. 4a). Quantification of the corresponding bands by densitometry showed that the relative furin abundances in these five cell lines are 293T (0.04), A549 (0.18), HeLa (0.29), H1299 (0.56) and Huh7 (treated as 1) (Fig. 4a). Due to the lack of specificity, the furin antibody used failed to detect the protein in Vero and other cells of animal origin (data not shown).

Interestingly, the two cell lines, Huh7 and H1299, with high levels of furin expression are highly permissive to IBV and support productive IBV infection. To study further the infection kinetics of IBV infection and to compare the viral infectivity in these cells, the same number of cells (2×10^6) was plated. After incubation for 14 h, cells were infected with IBV-Luc at a multiplicity of infection of approximately 2, harvested at 24 h post-infection, and the luciferase activities were measured (Shen et al., 2009). The highest readings were consistently obtained from IBV-infected Huh7 cells, and were considered as 100% infection efficiency for each passage of IBV in this cell line, and the readings in other cells were shown as percentages of that in Huh7 cells (Fig. 4b). Compared to IBV-infected Huh7 cells, the percentages of the relative luciferase activity (relative IBV infectivity) in IBV-infected H1299, 293T, HeLa and A549 cells are 68.55, 19.32, 9.15 and 0.88%, respectively, at passage 1 (Fig. 4b). At passage 2, the percentages were reduced to 26.29, 0.12, 0.46 and 0%, respectively, in IBV-infected H1299, 293T, HeLa and A549 cells (Fig. 4b). At passage 5, the percentage in H1299 cells is 32.94%, and no infection was observed in the other three cell lines (Fig. 4b). Based on the luciferase reading, IBV replication in H1299 cells at passages 2 and 5 appeared to be much reduced, compared to that in passage 1. However, no obvious reduction in IBV replication was observed when the virus was continuously propagated in this cell line, based on the growth curves shown in Fig. 3b. The reason for this discrepancy is currently unclear, but it may reflect the intrinsic differences of the two assays, that is, the luciferase assay is to measure the viral replication and protein synthesis in the cell and the growth curve is to measure the production of infectious virus particles.

The furin abundance in other three human cell lines, Hep3B, HepG2 and HCT116, with varying susceptibilities to IBV was analyzed by Western blot. Once again, differential expression of furin in these cells was observed. Compared with the furin level in Huh7 (treated as 1), the relative furin abundances in these cells are Hep3B (0.6), HCT116 (0.13) and HepG2 (0.28), as determined by densitometry (Fig. 4c). The data largely correlate with the permissiveness of these cell lines to productive IBV infection, with HepG2 cells as one exception, which was shown to have an intermediate level of furin. The reason why HepG2 cells could support efficient productive IBV infection but are with a relatively low furin abundance is currently unclear. It would point to the involvement of multiple host cell factors in either restriction or promotion of IBV infection and is worthy of further studies.

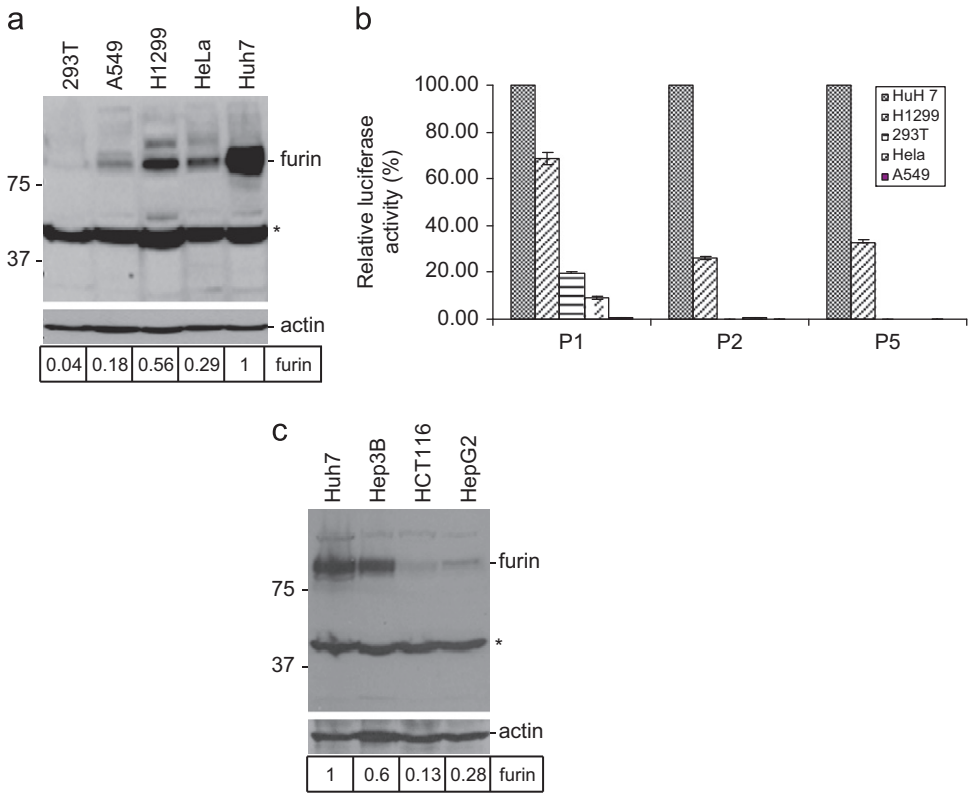

Fig. 4. Correlation between cellular furin content and productive IBV infection in five human cell lines. (a) Western blot analysis of the furin abundance in 293 T, A549, H1299, HeLa and Huh7 cells. Total lysates were prepared and separated on SDS-12% polyacrylamide gels. The expression of furin was analyzed by Western blot with anti-furin antibodies. The furin band (furin) and an unknown band (*) are indicated. The membrane was also probed with anti-actin monoclonal antibody as a loading control. The relative furin abundance in these cells is shown as the fraction of the furin abundance in Huh7 cells, which was arbitrarily defined as 1. (b) Productive IBV infection in 293T, A549, H1299, HeLa and Huh7 cells. 2×10^6 cells in duplicate were plated and infected with IBV-Luc at a multiplicity of infection of approximately 2. Cells were harvested at 24 h post-infection and virus stocks were prepared from one set of cells by freezing and thawing and used to infect fresh cells. The luciferase activities were measured from the other set of cells and the readings from IBV-infected Huh7 cells were considered as 100% infection efficiency for each passage. The readings in other cells were shown as percentages of that in Huh7 cells. (c) Western blot analysis of the furin abundance in Hep3B, HCT116, HepG2 and Huh7 cells. Total lysates were prepared and separated on SDS-12% polyacrylamide gels. The expression of furin was analyzed by Western blot with anti-furin antibodies. The furin band (furin) and an unknown band (*) are indicated. The membrane was also probed with anti-actin monoclonal antibody as a loading control. The relative furin abundance in these cells is shown as the fraction of the furin abundance in Huh7 cells, which was arbitrarily defined as 1.

Ablation of productive IBV infection by knockdown of furin expression in H1299 cells

Knockdown of furin by siRNA in both Huh7 and H1299 cells was then carried out to test further if productive IBV infection is correlated with the furin abundance in each cell line. As shown in Fig. 5a, introduction of siRNA duplexes targeting furin into H1299 cells significantly reduced the furin expression at the protein level. However, only a marginal effect was achieved in Huh7 cells (Fig. 5a), probably reflecting the poorer transfection efficiency in this cell line. Infection of these cells with IBV at a multiplicity of infection of approximately 1 showed formation of much smaller sycyntia in furin-knockdown H1299 cells at 20 h post-infection, compared to the control cells transfected with siRNA targeting EGFP (Fig. 5b). Continuous propagation of IBV prepared from the same set of furin-knockdown and control cells led to a loss of viral infectivity from the second passage onward in furin-knockdown H1299 cells, but not in H1299 cells treated with siEGFP and Huh7 cells treated with siEGFP and siFurin, respectively (Fig. 5c). More S protein was expressed in Huh7 cells transfected with siEGFP than did in siFurin-transfected cells, probably due to their relative higher furin abundance, which would in turn enhance viral infection (Fig. 5c). Interestingly, higher expression of IBV S protein was detected in passage 2 of IBV-infected Huh7 cells treated with either siFurin or siEGFP than that in passage 1 (Fig. 5c), correlating with the highest expression level of furin in this cell line. Taken together, these results confirm that the abundant expression of furin is one of the factors that support productive IBV infection in cultured cells.

Enhancement of productive IBV infection by knockin of furin in A549 cells

Five stable furin-knockin clones with different levels of furin expression were then selected from A549 cells (Fig. 6a). It was noted that stable clones with higher levels (clones 1, 3 and 5) of furin expression tended to round up and die soon after forming monolayers (data not shown), probably due to the harmful effect of high furin expression level in this cell line. Infection of these clones with IBV at passage 1 showed much more efficient viral infection, compared to that in wild type A549 cells (Fig. 6a). As shown in Fig. 6b, the formation of large syncytia at 24 h post-infection was seen in IBV-infected clones 4 and 5 at passage 1 (Fig. 6b). However, many rounded-up and dead cells were observed in IBV-infected clone 5 at 24 h post-infection (Fig. 6b). The same phenomenon was observed in other furin-knockin clones with an intermediate to high level of furin expression.

Continuous propagation of IBV in clones 4 and 5 was then carried out, showing efficient infection in wild type and the two stable clones at passage 1 (Fig. 6b and c). However, the infectivity was gradually attenuated in the subsequent passages and that the virus could be propagated up to passage 4 only in clone 4, but not in clone 5 due to massive death of the infected cells (Fig. 6b and c). IBV infection of clone 4 tends to show restricted CPE with the

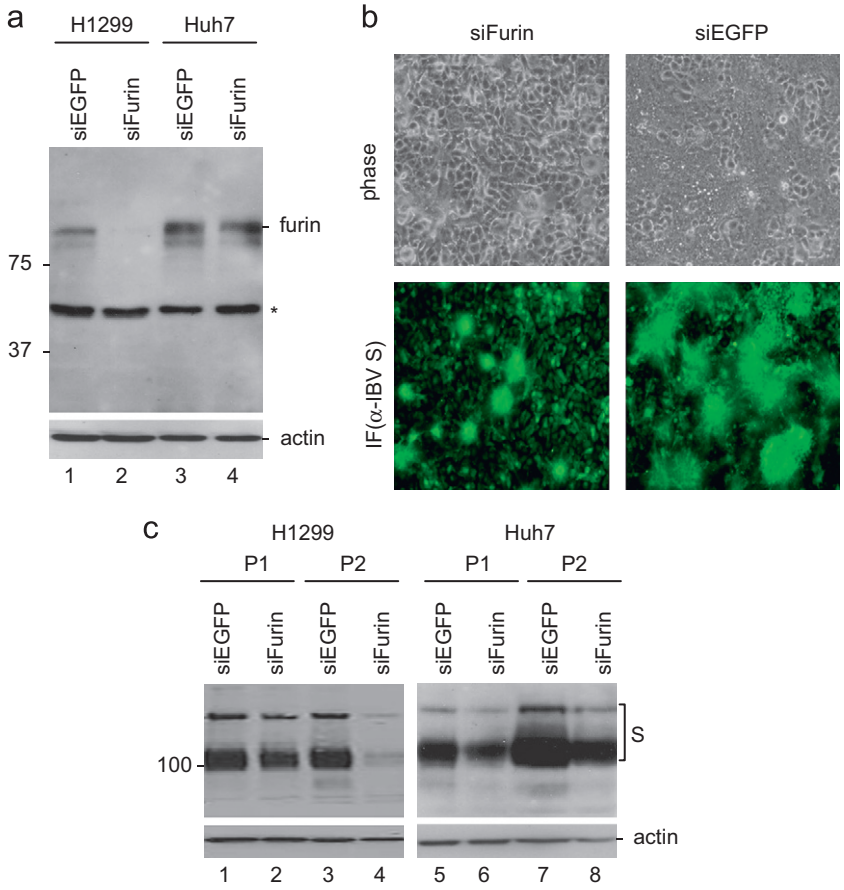

Fig. 5. Effects of furin-knockdown in Huh7 and H1299 cells on productive IBV infection. (a) Knockdown of furin by siRNA in H1299 and Huh7 cells. Cells were transfected with siRNA duplexes targeting either EGFP or Furin and were harvested 48 h post-transfection. Total lysates were prepared and separated on SDS-12% polyacrylamide gels. The expression of furin was analyzed by Western blot with anti-furin antibodies. The membrane was also probed with anti-actin monoclonal antibody as a loading control. (b) Effect of furin-knockdown on syncytium formation in IBV-infected H1299 cells. H1299 cells were transfected with siRNA duplexes targeting either EGFP or Furin, and infected with IBV at a multiplicity of infection of approximately 1 at 24 h post-transfection. Cells were observed under microscopy at 24 h post-infection. The cells were then fixed and stained with anti-IBV S antibodies. (c) Effect of furin-knockdown on productive IBV infection in H1299 and Huh7 cells. H1299 and Huh7 cells were transfected with siRNA duplexes targeting either EGFP or Furin, and infected with IBV at a multiplicity of infection of approximately 1 at 24 h post-transfection. Total cell lysates prepared from p1 and p2 infected cells were separated on SDS-12% polyacrylamide gels and analyzed by Western blot with ant-IBV S antibodies. The membrane was also probed with anti-actin monoclonal antibody as a loading control.

infected cells died and detached from the dishes afterward (Fig. 6b). This result reveals the harmful effect of higher furin expression level and indicates that additional factor(s) may be required for efficient productive infection of IBV in this cell line.

The effect of furin abundance on IBV infection was further studied by transfection of furin into 293T cells, followed by infection of the transfected cells with IBV at a multiplicity of infection of approximately 1. As shown in Fig. 6d, overexpression of furin in 293T cells resulted in the detection of approximately 2-fold more N protein (Fig. 6d). Titration of the virus particles released to the culture media showed 4.2-fold more infectious virus particles were released from cells overexpressing furin.

Analysis of IBV S protein cleavage at the two confirmed furin-cleavage sites in Huh7, H1299, HeLa, A549 and 293T cells

After demonstrating the relationship between the cellular furin abundance and the productive IBV infection in Huh7, H1299, HeLa, A549 and 293T cells, the cleavage efficiency of IBV S protein by furin at the two identified furin sites in these cell lines was then studied by transfection with appropriate S constructs and infection with IBV, respectively. First, Huh7, H1299, HeLa, A549 and 293T cells were transfected with S(1–789)Fc construct (Fig. 7a) (Yamada and Liu, 2009), and analyzed by Western blot with human IgG. Expression of S(1–789)Fc in H1299 and Huh7 led to efficient cleavage of S-Fc fusion protein at both R_{537}/S (cl-1C) and R_{690}/S (cl-2C) positions (Fig. 7b). Much weaker cleavage could be detectable in HeLa after prolong exposure of the gel (data not shown). No obvious cleavage of the fusion protein at the two positions was detected when the construct was expressed in 293T and A549 cells (Fig. 7b), revealing the correlation between the low furin abundance and the lack of S protein proteolysis in these cells.

Huh7, HeLa, A549 and Vero cells were then infected with a recombinant IBV expressing a Flag-tagged S protein (IBVS-Flag539) (Fig. 7a) (Yamada and Liu, 2009). In addition to the detection of the full-length S protein (S-Flag539), products derived from single cleavage at R_{537}/S (cl-1C) and R_{690}/S (cl-2N) sites as well as dual cleavage (cl-dual) were clearly detected in Huh7 and Vero cells infected with the recombinant virus (Fig. 7c). The percentages of the three cleavage products were 15, 43 and 32%, respectively in Vero cells, and 14, 43 and 34%, respectively, in Huh7 cells (Fig. 7c). The same set of cleavage products was also detected, although with much reduced efficiency, in HeLa cells infected with the recombinant IBV (Fig. 7c). The percentages of the three cleavage products were 16, 22 and 8%, respectively, in this cell line (Fig. 7c). However, no cleavage bands were detected in A549 cells infected with the same virus (Fig. 7c). Taken together, these results suggest that the correlation between the cellular furin abundance and the productive IBV infection in

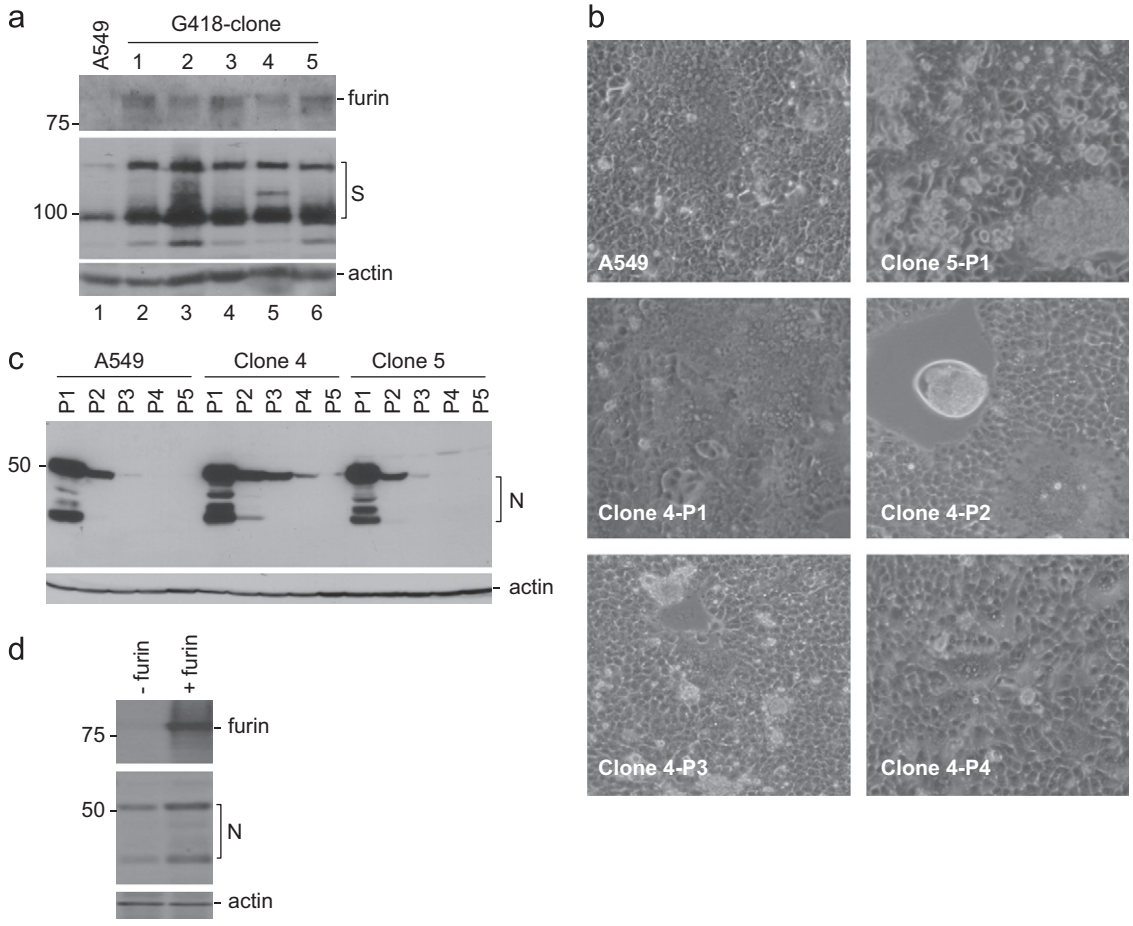

Fig. 6. Effects of furin-knockin in A549 cells on productive IBV infection. (a) Selection of furin-knockin clones and the effect on productive IBV infection in A549 cells. Wild type A549 cells and five G418-selected clones with furin-knockin were selected and infected with IBV at a multiplicity of infection of approximately 1, and harvested at 24 h post-infection. Total cell lysates were prepared, separated on SDS-10% polyacrylamide gels and analyzed by Western blot with anti-furin and anti-IBV S antibodies. The same membranes were also probed with anti-actin antibodies. (b) Syncytium formation in furin-knockin A549 cells infected with IBV. Wild type A549 cells and the two furin-knockin cells (clones 4 and 5) were infected with IBV at a multiplicity of infection of approximately 1 and virus stocks were prepared by freezing/thawing the infected cells three times at room temperature at 24 h post-infection. Continuous propagation was carried out by infection of fresh cell monolayers with the virus stocks. The formation of syncytia was observed under the microscope at 24–48 h post-infection. (c) Effect of furin-knockin on productive IBV infection in A549 and furin-knockin clones. Total cell lysates prepared from p1 to p5 infected cells, separated on SDS-12% polyacrylamide gels and analyzed by Western blot with ant-IBV N antibodies. The membrane was also probed with anti-actin monoclonal antibody as a loading control. (d) Effect of overexpression of furin on IBV infection in 293 T cells. Cells were transfected with furin, and infected with IBV stocks prepared from IBV-infected Vero cells at a multiplicity of infection of approximately 1 at 14 h post-transfection. Cells were harvested at 24 h post-infection, lysates prepared, separated on SDS-10% polyacrylamide gels and analyzed by Western blot with anti-furin and anti-IBV N antibodies. The same membranes were also probed with anti-actin antibodies.

different cells may be due to a differential efficiency of S protein cleavage mediated by furin. As cleavage of IBV S protein at the first furin site (R_{537}/S) was shown to be nonessential for the replication and infectivity of IBV in cultured cells (Yamada and Liu, 2009; Yamada et al., 2009), acquisition of the second furin site (R_{690}/S) during adaptation of IBV Beaudette strain from chicken embryo to cell culture system may be essential for the adaptation process.

Discussion

Coronavirus is generally believed to have a narrow range of host specificity. For example, chicken is the only natural host for IBV, although IBV was also isolated from pheasants as well (Gough et al., 1996). Clinical and field isolates of IBV can only be propagated either in embryonated chicken eggs or transiently in primary chicken embryo kidney cells. IBV Beaudette-42 and Holte strains could grow in BHK-21 cell line (Otsuki et al., 1979), and the Beaudette strain of IBV from chicken embryo was adapted to Vero cells (Shen et al., 2003, 2004). More recently, IBV was shown to infect HeLa cells depending on the status of the cells (Chen et al., 2007). However, the susceptibility of other cell lines to IBV has not been documented. In this study, cell lines of diverse species and tissue origins were shown to be susceptible to the Vero-adapted IBV. The virus was efficiently propagated in four human cell lines, including H1299, HepG2, Hep3B and Huh7, for at least 20 passages. Among the four cell lines, HepG2, Hep3B, and Huh7 cell lines are derived from human hepatoma, and H1299 cells are human cancer cells of lung origins, respectively. Continuous propagation of the Vero-adapted IBV in human cells showed no further accumulation of mutations in the S protein. The fact that IBV has gained the ability to infect human and other animal cells once adapted to Vero cells suggests that adaptation of IBV to a monkey kidney cell line may allow the virus to cross not only species but also tissue barriers.

The presence of cellular receptor(s) in a particular cell line is a pre-requisite for the establishment of successful infection by a virus. Although the cellular receptor(s) for IBV is yet to be firmly established, association of cell-surface sialic acid and a low-pH environment were reported to be required for IBV entry (Chu et al., 2006; Winter et al., 2006, 2008). The observation that most

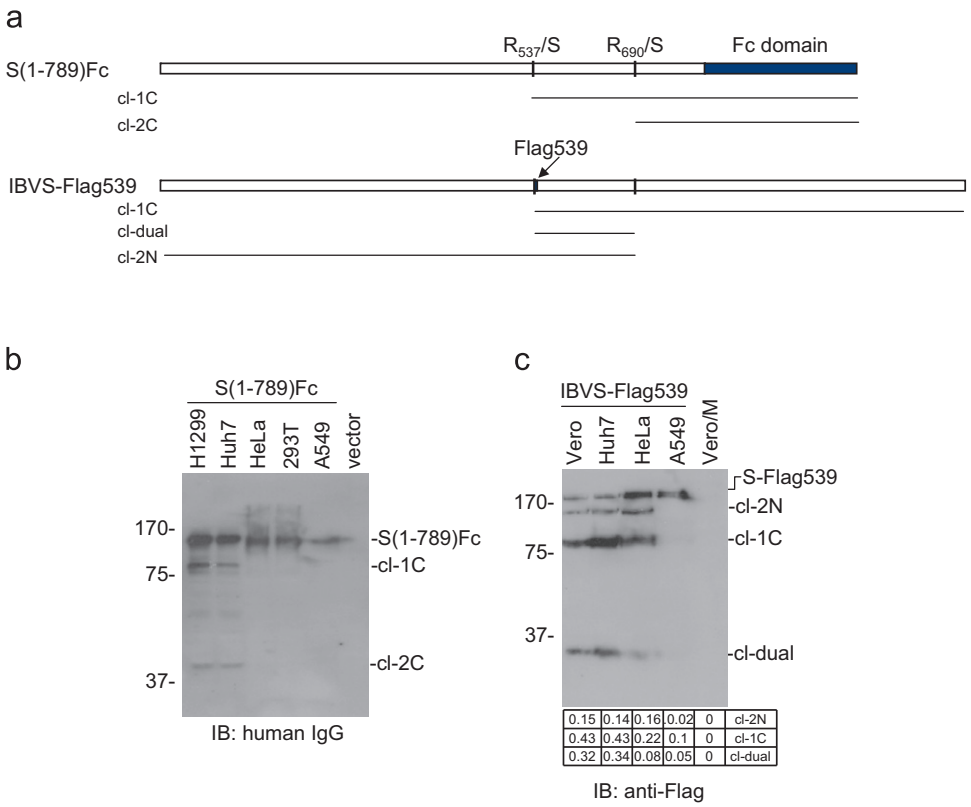

Fig. 7. Differential efficiency in proteolysis of IBV S protein at the two confirmed furin-cleavage sites in Huh7, H1299, HeLa, A549 and 293T cells. (a) Diagram of S(1–789)Fc construct and a recombinant IBV (IBV-Flag539) expressing a Flag tag inserted into IBV S protein at amino acid position 539. The positions of first (R_{690}/S) and second (R_{690}/S) furin sites, the sites for the Fc domain and the Flag tag, and the cleavage products are shown. (b) Expression and cleavage of S(1–789)Fc in Huh7, H1299, HeLa, A549 and 293 T cells. Cells were transfected with S(1–789)Fc construct, total lysates prepared and separated on SDS-12% polyacrylamide gels. The expression and processing of the S-Fc fusion protein were analyzed by staining the membrane with an anti-human IgG antibody. Products derived from cleavage of S-Fc fusion protein at R_{537}/S (cl-1C) R_{690}/S (cl-2C) as well as the full-length product (S(1–789)Fc are indicated. (c) Expression and proteolysis of S protein in Huh7, HeLa, A549 and Vero cells infected with IBVS-Flag539. Cells were infected with IBVS-Flag539 at a multiplicity of infection of approximately 2 and harvested at 18 h post-infection. Total cell lysates prepared from p1 and p2 infected cells were separated on SDS-15% polyacrylamide gels and analyzed by Western blot with ant-Flag antibodies. Products derived from single cleavage at R_{537}/S (cl-1C), R_{690}/S (cl-2N), dual cleavage (cl-dual) and the full-length Flag-tagged S protein (S-Flag539) are indicated. The percentages of the three cleavage products, cl-2N, cl-1C and cl-dual, were also calculated and shown.

cell lines tested in this study could support efficient IBV infection in passage 1 suggests that the Vero-adapted IBV is able to enter and replicate efficiently in these cells, but cannot support productive IBV infection, pointing to the possibility that additional host factors are required to enhance the infectivity and to promote productive IBV infection in these cells.

Another important host cell restriction point may be at the release of progeny viruses from initially infected cells and spread of the primary infection to the neighboring cells. Generally, IBV is not efficiently released to the culture medium even in highly permissive cells. When most cell lines were initially infected with Vero-adapted IBV, relatively efficient infection was observed. During subsequent passages of the virus in the more resistant cells, however, the viral infectivity was gradually attenuated and totally lost after less than five passages. Slightly less efficient IBV infection was even observed in H1299 cells transfected with siEGFP in passage 2, although the same treated H1299 cells could support productive IBV infection. As the initial virus stocks were prepared by freezing and thawing IBV-infected Vero cells, most infectious virus particles may be still associated with cellular membranes and cell debris from Vero cells. The presence of certain amounts of host enhancement factor(s) in these initial virus stocks may help to establish efficient infection during initial propagation of IBV in the less permissive cell lines. In fact, much less infection was observed in some of these cells when clarified virus stocks harvested from the culture media of IBV-infected Vero cells were used (data not shown), supporting the argument that cellular membranes and cell debris from Vero cells contained in the initial virus stocks may enhance IBV-infection of these less permissive cell lines during passage 1.

In this study, a membrane-bound cellular proprotein convertase, furin, is identified as a host cell factor that may enhance the productive IBV infection in cultured cells. Among the five cell lines tested in this study, Huh7 cells have the highest furin expression level, followed by H1299 cells. Both cell lines could support efficient virus replication and productive infection. HeLa cells, with an intermediate level of furin expression, were shown to be susceptible to IBV infection under certain circumstances (Chen et al., 2007), consistent with the observation in this study that a certain level of furin-mediated cleavage of S protein was observed in IBV-infected HeLa cells. Under the experimental conditions used in this study, this cell line could support productive IBV infection up to passage 4. The other two cell lines, A549 and 293T, have the lowest furin expression level and can be efficiently infected in passage 1 only; the infectivity dropped to almost undetectable levels in passage 2. It was noted that quite efficient infection occurs in 293T cells in passage 1, probably because 293T cells grow fast and tend to form large cell clumps as well as more compact lawns, which may facilitate coronavirus infection (Snijder et al., 2009). Nevertheless, the facts that cellular furin content is nicely correlated with viral infectivity and productive IBV infection in these five human cell lines and that knockdown of furin by siRNA in H1299 aborts productive IBV infection provide solid evidence supporting the conclusion that

furin is one of the host factors required for the establishment of productive IBV infection. The less consistent observations generated from G418-resistant furin-knockin A549 cell clones infected with IBV, on the other hand, point to the possibility that additional cellular factors are also involved in this process. In fact, it was recently reported that several cellular factors are actively involved in the IBV replication cycle. These include DDX1, MADP1 (zinc finger CCHC-type and RNA binding motif 1) and DNA polymerase delta (Tan et al., 2012; Xu et al., 2010, 2011). It is yet to be determined if the variation in the cellular contents of these proteins may also contribute to the replication efficiency of IBV in individual cell lines.

The furin-mediated enhancement effect on productive IBV infection would be realized either by acceleration of viral spread during primary infection or by promoting entry of the viruses released from the primary infection in the same passage. The exact role of furin in enhancement of cell permissiveness to IBV infection is less clear. As furin-mediated cleavage of S protein at the second furin site was shown to play an important role in viral infectivity by promoting virus–cell and cell–cell fusion (Yamada and Liu, 2009), it would be reasonable to speculate that furin may facilitate viral entry and spread. In this regard, subtle differences in expression of furin in different tissues and cells may explain why IBV infects one tissue but not another, although it is believed that furin is ubiquitously expressed (Bosshart et al., 1994; Molloy et al., 1994). Further studies of the furin expression and distribution patterns in chicken and utilization of recombinant IBV containing sequences from different pathogenic IBV strains would provide more insights into IBV pathogenesis and cell and tissue tropisms.

Materials and methods

Viruses and cell lines

The Beaudette strain of IBV was purchased from ATCC and propagated in chicken embryonated eggs for three passages. The viruses were then adapted to grow and passage on Vero cells for 65 passages at 37 °C and used to infect other cell lines (Shen et al., 2003; Liu et al., 1995).

A549 (ATCC CCL-185), BHK-21 (ATCC CCL-10), CHO (ATCC CCL-61), HeLa (ATCC CCL-2), HepG2 (ATCC HB-8065), Hep3B (ATCC HB-8064), Huh-7 (JCRB0403), 293T (ATCC, CRL-11268) and Vero (ATCC CCL-81) cells were maintained in complete DMEM medium (JRH) supplemented with 10% newborn calf serum. Cos-7 (ATCC CRL-1651), H1299 (ATCC CRL-5803), DLD-1 (ATCC CCL-221), DLD-1 clone A (DLD-1A) and U-937 (ATCC CRL-1593.2) cells were maintained in complete RPMI 1640 medium (JRH) supplemented with 10% newborn calf serum. HCT116 (ATCC CCL-247) cells were maintained in complete McCoy's 5a medium (Sigma) supplemented with 10% newborn calf serum.

Plaque purification of virus

Viral stocks were 10-fold serially diluted and 200 μl of the diluted virus stocks were added dropwise to the monolayer of cells grown on 6-well plates with gentle swirling. Viruses were allowed to infect cells for 2 h at 37 °C, 5% humidified CO_2, with occasional shaking. After the inoculum was removed, the cells were washed twice with 1 × PBS, and the monolayers were overlaid with 1.5 ml DMEM containing 1% cell-culture grade, low temperature melting agarose. The plates were left at room temperature for about 15 min and then incubated at 37 °C, 5% humidified CO_2 for 4–7 day until the plaques were grown up. Individual plaques were selected and inoculated to fresh cell monolayers for amplification.

Western blot analysis

After SDS–PAGE, proteins were transferred to nitrocellulose membrane (Bio-Rad) with a semidry transfer cell (Bio-Rad Trans Blot SD). The membrane was blocked overnight at 4 °C in blocking buffer containing 5% non-fat milk in TBST (20 mM Tris-HCl, pH 7.4, 150 mM NaCl, 0.1% Tween-20), incubated with specific antiserum diluted in blocking buffer (1:500–1:2000) at room temperature for 2 h, washed three times with TBST, and incubated with horseradish peroxidase-conjugated anti-rabbit or anti-mouse immunoglobulin (DAKO) diluted in blocking buffer (1:2000) at room temperature for 1 h. Proteins were detected using the enhanced chemiluminescence (ECL) detection reagents (Amersham, UK).

Growth curve of IBV on Vero cells

Cells were infected with the Vero-adapted IBV, and harvested at different time points post-infection. Virus stocks were prepared by freezing/thawing of the infected cells three times. The 50% tissue culture infection dose (TCID50) of each sample was determined, as previously described, by infecting five wells of Vero cells on 96-well plates in duplicate with 10-fold serial dilution of each virus stock (Xu et al., 2010).

Immunofluorescent (IF) staining

Cells were cultivated in 24-well plates and infected with IBV. The infected cells were washed with phosphate buffered saline (PBS) supplemented with 10% goat serum, fixed with 4% paraformaldehyde in PBS for 15 min, and permeabilized with 0.2% Triton X-100 for 10 min. IF staining was performed by incubating cells with anti-IBV S antibodies and subsequently with the FITC-conjugated anti-rabbit IgG. Cells were examined by fluorescent microscopy.

RNA interference and selection of stable cells with knockin or knockdown of a gene

Cells with 60% confluence were grown on 6-well plates and transfected with 20 nM of siRNA duplexes targeting either furin (5′–GGACUAAACGGGACGUGUA-3′) or EGFP (5′–GCAACGUGACC-CUGAAGUUC-3) with Lipofectamine™ RNAiMAX (Invitrogen). At 24 h post-transfection, cells were infected with IBV at a multiplicity of infection of approximately 2.

The furin coding region was amplified by RT-PCR, and the PCR fragment was cloned into a mammalian expression vector with a neomycin selection marker, and transfected into cells. At 24 h post-transfection, 1 mg/ml of G418 was added to the medium. At a 3-day interval, the medium was replaced with fresh medium containing the same concentration of G418. G418-resistant clones were picked approximately 30 day later and amplified. The amplified cell clones were harvested and analyzed by Northern and Western blot analyses. Clones with different levels of furin expression were selected for subsequent studies.

References

Belouzard, S., Chu, V.C., Whittaker, G.R., 2009. Activation of the SARS coronavirus spike protein via sequential proteolytic cleavage at two distinct sites. Proc. Natl. Acad. Sci. U.S.A. 106 (14), 5871–5876.

Bosshart, H., Humphrey, J., Deignan, E., Davidson, J., Drazba, J., Yuan, L., Oorschot, V., Peters, P.J., Bonifacino, J.S., 1994. The cytoplasmic domain mediates

localization of furin to the trans-Golgi network en route to the endosomal/lysosomal system. J. Cell Biol. 126, 1157–1172.
Butler, N., Pewe, L., Trandem, K., Perlman, S., 2006. Murine encephalitis caused by HCoV-OC43, a human coronavirus with broad species specificity, is partly immune-mediated. Virology 347, 401–421.
Cavanagh, D., 2007. Coronavirus avian infectious bronchitis virus. Vet. Res. 38, 281–297.
Chen, H.Y., Guo, A.Z., Peng, B., Zhang, M.F., Guo, H.Y., Chen, H.C., 2007. Infection of HeLa cells by avian infectious bronchitis virus is dependent on cell status. Avian Pathol. 36, 269–274.
Chu, V.C., McElroy, L.J., Chu, V., Bauman, B.E., Whittaker, G.R., 2006. The avian coronavirus infectious bronchitis virus undergoes direct low-pH-dependent fusion activation during entry into host cells. J. Virol. 80, 3180–3188.
Coutelier, J.P., Godfraind, C., Dveksler, G.S., Wysocka, M., Cardellichio, C.B., Noel, H., Holmes, K.V., 1994. B lymphocyte and macrophage expression of carcinoembryonic antigen-related adhesion molecules that serve as receptors for murine coronavirus. Eur. J. Immunol. 24, 1383–1390.
Curtis, B.M., Scharnowske, S., Watson, A.J., 1992. Sequence and expression of a membrane-associated C-type lectin that exhibits CD4-independent binding of human immunodeficiency virus envelope glycoprotein gp120. Proc. Natl. Acad. Sci. U.S.A. 89, 8356–8360.
Delmas, B., Gelfi, J., L'Haridon, R., Vogel, L.K., Sjostrom, H., Noren, O., Laude, H., 1992. Aminopeptidase N is a major receptor for the entero-pathogenic coronavirus TGEV. Nature 357, 417–420.
Dveksler, G.S., Pensiero, M.N., Cardellichio, C.B., Williams, R.K., Jiang, G.S., Holmes, K.V., Dieffenbach, C.W., 1991. Cloning of the mouse hepatitis virus (MHV) receptor: expression in human and hamster cell lines confers susceptibility to MHV. J. Virol. 65, 6881–6891.
Fang, S.G., Chen, B., Tay, F.P.L., Liu, D.X., 2007. An arginine-to-proline mutation in a domain with undefined functions within the helicase protein (NSP13) is lethal to the coronavirus infectious bronchitis virus in cultured cells. Virology 358, 136–147.
Fang, S.G., Shen, S., Tay, F.P.L., Liu, D.X., 2005. Selection of and recombination between minor variants lead to the adaptation of an avian coronavirus to primate cells. Biochem. Biophys. Res. Commun. 336 (417–423).
Geijtenbeek, T.B., Kwon, D.S., Torensma, R., van Vliet, S.J., van Duijnhoven, G.C., Middel, J., Cornelissen, I.L., Nottet, H.S., KewalRamani, V.N., Littman, D.R., Figdor, C.G., van Kooyk, Y., 2000. DC-SIGN, a dendritic cell-specific HIV-1-binding protein that enhances trans-infection of T cells. Cell 100, 587–597.
Godfraind, C., Langreth, S.G., Cardellichio, C.B., Knobler, R., Coutelier, J.P., Dubois-Dalcq, M., Holmes, K.V., 1995. Tissue and cellular distribution of an adhesion molecule in the carcinoembryonic antigen family that serves as a receptor for mouse hepatitis virus. Lab. Invest. 73, 615–627.
Gough, R.E., Cox, W.J., Winkler, C.E., Sharp, M.W., Spackman, D., 1996. Isolation and identification of infectious bronchitis virus from pheasants. Vet. Rec. 138, 208–209.
Guan, Y., Zheng, B.J., He, Y.Q., Liu, X.L., Zhuang, Z.X., Cheung, C.L., Luo, S.W., Li, P.H., Zhang, L.J., Guan, Y.J., Butt, K.M., Wong, K.L., Chan, K.W., Lim, W., Shortridge, K.F., Yuen, K.Y., Peiris, J.S., Poon, L.L., 2003. Isolation and characterization of viruses related to the SARS coronavirus from animals in southern China. Science 302, 276–278.
Halary, F., Amara, A., Lortat-Jacob, H., Messerle, M., Delaunay, T., Houlès, C., Fieschi, F., Arenzana-Seisdedos, F., Moreau, J.F., Déchanet-Merville, J., 2002. Human cytomegalovirus binding to DC-SIGN is required for dendritic cell infection and target cell trans-infection. Immunity 17, 653–664.
Hofmann, H., Pyrc, K., van der Hoek, L., Geier, M., Berkhout, B., Pohlmann, S., 2005. Human coronavirus NL63 employs the severe acute respiratory syndrome coronavirus receptor for cellular entry. Proc. Natl. Acad. Sci. U.S.A. 102, 7988–7993.
Jeffers, S.A., Tusell, S.M., Gillim-Ross, L., Hemmila, E.M., Achenbach, J.E., Babcock, G.J., Thomas Jr, W.D., Thackray, L.B., Young, M.D., Mason, R.J., Ambrosino, D.M., Wentworth, D.E., Demartini, J.C., Holmes, K.V., 2004. CD209L (L-SIGN) is a receptor for severe acute respiratory syndrome coronavirus. Proc. Natl. Acad. Sci. U.S.A. 101, 15748–15753.
Li, F.Q., Xiao, H., Tam, J.P., Liu, D.X., 2005. Sumoylation of the nucleocapsid protein of severe acute respiratory syndrome coronavirus. FEBS Lett. 579, 2387–2396.
Li, W., Moore, M.J., Vasilieva, N., Sui, J., Wong, S.K., Berne, M.A., Somasundaran, M., Sullivan, J.L., Luzuriaga, K., Greenough, T.C., Choe, H., Farzan, M., 2003. Angiotensin-converting enzyme 2 is a functional receptor for the SARS coronavirus. Nature 426, 450–454.
Liu, D.X., Tibbles, K.W., Cavanagh, D., Brown, T.D.K., Brierley, I., 1995. Identification, expression and processing of an 87 K polypeptide encoded by ORF1a of the coronavirus infectious bronchitis virus. Virology 208, 48–57.
Miguel, B., Pharr, G.T., Wang, C., 2002. The role of feline aminopeptidase N as a receptor for infectious bronchitis virus. Arch. Virol. 147, 2047–2056.
Molloy, S.S., Thomas, L., VanSlyke, J.K., Stenberg, P.E., Thomas, G., 1994. Intracellular trafficking and activation of the furin proprotein convertase: localization to the TGN and recycling from the cell surface. EMBO J. 13, 18–33.
Otsuki, K., Noro, K., Yamamoto, H., Tsubokura, M., 1979. Studies on avian infectious bronchitis virus (IBV). II. Propagation of IBV in several cultured cells. Arch. Virol. 60, 115–122.
Pohlmann, S., Zhang, J., Baribaud, F., Chen, Z., Leslie, G.J., Lin, G., Granelli-Piperno, A., Doms, R.W., Rice, C.M., McKeating, J.A., 2003. Hepatitis C virus glycoproteins interact with DC-SIGN and DC-SIGNR. J. Virol. 77, 4070–4080.
Shen, H., Fang, S.G., Chen, B., Chen, G., Tay, F.P., Liu, D.X., 2009. Towards construction of viral vectors based on avian coronavirus infectious bronchitis virus for gene delivery and vaccine development. J. Virol. Methods 160, 48–56.
Shen, S., Law, Y.C., Liu, D.X., 2004. A single amino acid mutation in the spike protein of coronavirus infectious bronchitis virus hampers its maturation and incorporation into virions at the nonpermissive temperature. Virology 326, 288–298.
Shen, S., Wen, Z.L., Liu, D.X., 2003. Emergence of a coronavirus infectious bronchitis virus mutant with a truncated 3b gene: functional characterization of the 3b protein in pathogenesis and replication. Virololgy 311, 16–27.
Snijder, B., Sacher, R., Rämö, P., Damm, E.M., Liberali, P., Pelkmans, L., 2009. Population context determines cell-to-cell variability in endocytosis and virus infection. Nature 461, 520–523.
Tassaneetrithep, B., Burgess, T.H., Granelli-Piperno, A., Trumpfheller, C., Finke, J., Sun, W., Eller, M.A., Pattanapanyasat, K., Sarasombath, S., Birx, D.L., Steinman, R.M., Schlesinger, S., Marovich, M.A., 2003. DC-SIGN (CD209) mediates dengue virus infection of human dendritic cells. J. Exp. Med. 197, 823–829.
Tan, Y.W., Hong, W., Liu, D.X., 2012. Binding of the 5′-untranslated region of coronavirus RNA to zinc finger CCHC-type and RNA binding motif 1 enhances viral replication and transcription. Nucleic Acids Res. 40, 5065–5077.
Tresnan, D.B., Levis, R., Holmes, K.V., 1996. Feline aminopeptidase N serves as a receptor for feline, canine, porcine, and human coronaviruses in serogroup I. J. Virol. 70, 8669–8674.
Williams, R.K., Jiang, G.S., Holmes, K.V., 1991. Receptor for mouse hepatitis virus is a member of the carcinoembryonic antigen family of glycoproteins. Proc. Natl. Acad. Sci. U.S.A. 88, 5533–5536.
Winter, C., Schwegmann-Wessels, C., Cavanagh, D., Neumann, U., Herrler, G., 2006. Sialic acid is a receptor determinant for infection of cells by avian infectious bronchitis virus. J. Gen. Virol. 87, 1209–1216.
Winter, C., Herrler, G., Neumann, U., 2008. Infection of the tracheal epithelium by infectious bronchitis virus is sialic acid dependent. Microbes Infect. 10, 367–373.
Xu, L., Khadijah, S., Fang, S., Wang, L., Tay, F.P., Liu, D.X., 2010. The cellular RNA helicase DDX1 interacts with coronavirus nonstructural protein 14 and enhances viral replication. J. Virol. 84, 8571–8583.
Xu, L.H., Huang, M., Fang, S.G., Liu, D.X., 2011. Coronavirus infection induces DNA replication stress partly through interaction of its nonstructural protein 13 with the p125 subunit of DNA polymerase delta. J. Biol. Chem. 286, 39546–39559.
Yamada, Y., Liu, D.X., 2009. Proteolytic activation of the spike protein at a novel RRRR/S motif is implicated in furin-dependent entry, syncytium formation, and infectivity of coronavirus infectious bronchitis virus in cultured cells. J. Virol. 83, 8744–8758.
Yamada, Y., Liu, X.B., Fang, S.G., Tay, P.L., Liu, D.X., 2009. Acquisition of cell–cell fusion activity by amino acid substitution in spike protein determines the infectivity of a coronavirus in cultured cells. PLoS ONE 4, e6130.
Yeager, C.L., Ashmun, R.A., Williams, R.K., Cardellichio, C.B., Shapiro, L.H., Look, A.T., Holmes, K.V., 1992. Human aminopeptidase N is a receptor for human coronavirus 229E. Nature 357, 420–422.
Zhang, Y., Buckles, E., Whittaker, G.R., 2012. Expression of the C-type lectins DC-SIGN or L-SIGN alters host cell susceptibility for the avian coronavirus, infectious bronchitis virus. Vet. Microbiol. 157, 285–293.